


Effect of a conductive layer on Fabry-Pérot resonances

P. A. Gusikhin¹, V. M. Muravev¹, K. R. Dzhikirba¹, A. Shuvaev², A. Pimenov² and I. V. Kukushkin¹

¹*Institute of Solid State Physics, RAS, Chernogolovka 142432, Russia*

²*Institute of Solid State Physics, Vienna University of Technology, 1040 Vienna, Austria*

 (Received 7 July 2021; revised 27 August 2021; accepted 31 August 2021; published 9 September 2021)

Using terahertz spectroscopy, we investigate resonant transmission through a dielectric slab with a conducting layer of varied mobility on one side. We observe the well-known Fabry-Pérot resonances in the transmission. Two fundamentally different regimes of the electrodynamic response of the system are established. In the clean limit, when the radiation frequency exceeds the carrier relaxation rate, $\omega\tau \gg 1$, the system exhibits a plasmonic response. As a result, there is a continuous shift in the Fabry-Pérot resonances with respect to the system parameters. By contrast, in the dirty regime, when $\omega\tau \ll 1$, there is an abrupt π shift in the resonance frequency, as the renormalized film resistance matches the impedance of free space. We find that under this condition, Fabry-Pérot oscillations disappear entirely over a broad frequency range. Such a matching effect might be of interest in various terahertz applications, for example, involving broadband filters or absorbers.

DOI: [10.1103/PhysRevB.104.115408](https://doi.org/10.1103/PhysRevB.104.115408)

I. INTRODUCTION

When electromagnetic radiation is incident on a dielectric slab of thickness d , its transmission exhibits a number of resonances $\omega_N = N\omega_d = Nc\pi/\sqrt{\varepsilon}d$ ($N = 0, 1, 2, \dots$) corresponding to the excitation of Fabry-Pérot modes [1,2]. Over the years, Fabry-Pérot interferometers and resonators have become some of the most widespread devices in modern optics, quantum radiophysics, and laser technologies [3]. The presence of a conducting layer on the surface of the slab leads to a significant modification of the Fabry-Pérot resonances [4–11]. In our study, we consider two types of conducting layers. First, we utilize a series of structures with a high-quality two-dimensional electron system (2DES) in an AlGaAs/GaAs heterostructure. The second type of structure has thin chromium films evaporated on top of the high-resistivity silicon substrates.

In the present paper, we show that the frequency response of the structures under study varies significantly depending on the value of the relaxation parameter $\omega\tau$ —the product of the frequency of incident electromagnetic radiation and the relaxation time, respectively. As long as $\omega\tau \gg 1$, the 2DES behaves as a 2D plasma. In this limit, the frequency of the Fabry-Pérot resonances gradually increases with the 2D density, practically independent of the relaxation time τ . Most importantly, we demonstrate that frequency ω_N/ω_d is unambiguously defined by the dimensionless retardation parameter $A = 2\omega_p/\omega_d$, which is equal to the ratio of renormalized plasma frequency ω_p to the discrete frequency of the Fabry-Pérot étalon $\omega_d/2$. The plasma frequency is given by the formula [12,13]

$$\omega_p = \sqrt{\frac{n_s e^2}{(\varepsilon - 1)\varepsilon_0 m^* d}}, \quad \omega_p \ll \frac{c}{\sqrt{\varepsilon}d}, \quad (1)$$

where n_s and m^* are the density and effective mass of the 2D electrons, and ε is the effective permittivity of the substrate.

Then, for example, the frequency of the zero Fabry-Pérot peak ($N = 0$) can be expressed as [14,15]

$$\omega_0 = \frac{\omega_d}{2} \frac{A}{\sqrt{1+A^2}}. \quad (2)$$

Hence, it follows that in the limit of a large substrate thickness or electron density, the $N = 0$ Fabry-Pérot peak continuously shifts in frequency from zero to $\omega_d/2$.

In the opposite limit of $\omega\tau \ll 1$, the film electrodynamics is governed by the dissipative Drude relaxation. We experimentally demonstrate that the frequency positions of Fabry-Pérot maxima are practically independent of the 2D conductivity σ_s . Interestingly, we discover a critical film conductivity $\sigma_s/(\varepsilon_0 c) = \sqrt{\varepsilon} - 1$ at which there is a disappearance of Fabry-Pérot oscillations due to the impedance match between the air and the substrate through the conducting film. This phenomenon is analogous to that used in optics in antireflection coatings. We propose interpreting the results obtained at $\omega\tau \ll 1$ based on the wave-impedance concept.

II. METHODS

The measurements have been carried out on two types of structures. The first set of samples includes a 20-nm-wide Al_{0.24}Ga_{0.76}As/GaAs/Al_{0.24}Ga_{0.76}As quantum well grown by molecular beam epitaxy on a GaAs substrate of thickness $d = 0.65$ mm. The original wafer is polished down to achieve the thickness $d = 0.2$ mm. Two wafers have a single 20-nm-wide quantum well hosting electrons with 2D densities of $n_s = 1.4 \times 10^{11}$ and 1.4×10^{12} cm⁻², with respective electron mobilities $\mu = 0.7 \times 10^6$ and 100×10^3 cm²/V s derived from high-frequency data. The third wafer contains five 20-nm-wide quantum wells spaced 60 nm apart, with a total electron density $n_s = 6.4 \times 10^{12}$ cm⁻² and electron mobility $\mu = 60 \times 10^3$ cm²/V s. The other set of samples has high-resistivity silicon substrates of thickness $d = 0.4$ mm, with

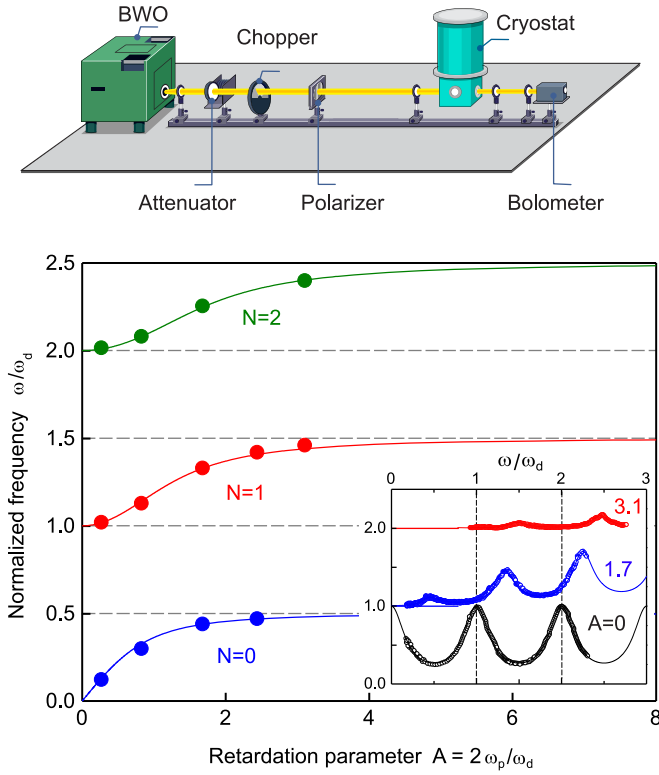


FIG. 1. Top panel: Schematics of the experimental setup. Bottom panel: Fabry-Pérot resonance frequency ω/ω_d as a function of the retardation parameter A . The inset depicts transmission data for three GaAs samples: $d = 0.2$ mm without 2DES (black circles, $A = 0$); $d = 0.19$ mm, $n_s = 6.4 \times 10^{12}$ cm $^{-2}$ (blue circles, $A = 1.7$); and $d = 0.65$ mm, $n_s = 6.4 \times 10^{12}$ cm $^{-2}$ (red circles, $A = 3.1$). For clarity, the curves are offset vertically by one unit.

a thin chromium film evaporated on one side. A 1×1 cm 2 sample is mounted on a sample holder with a 10 mm aperture at the location of the sample. Then, the sample is placed inside an optical cryostat. Continuous terahertz radiation from a set of backward-wave oscillators (BWOs) is applied normal to the sample surface, over the frequency range of 20–600 GHz. The transmitted power is measured by a He-cooled bolometer. All measurements are taken at the base sample temperatures of $T = 5$ and 300 K. The schematics of the experimental setup are shown in the top panel of Fig. 1. The details of the terahertz quasioptic experiment can be found elsewhere [16].

III. RESULTS

The inset to Fig. 1 displays the outcome of the transmission experiment at $T = 5$ K for three samples with different GaAs substrate thicknesses: $d = 0.65$ mm with no 2DES (black circles); $d = 0.19$ mm, $n_s = 6.4 \times 10^{12}$ cm $^{-2}$ (blue circles); and $d = 0.65$ mm, $n_s = 6.4 \times 10^{12}$ cm $^{-2}$ (red circles). The transmittance spectra are plotted versus the normalized frequency ω/ω_d , where $\omega_d = c\pi/\sqrt{\varepsilon_{\text{GaAs}}}d$ is the discrete frequency of the Fabry-Pérot étalon. The solid lines in the inset are the predictions of an analytical model based on the Drude dynamic conductivity in the quasiclassical approximation. For more details on the theoretical model, we refer the reader

to the Supplemental Material [17]. The resultant data suggest that a conducting 2DES layer significantly influences the frequency positions of the Fabry-Pérot peaks. Moreover, an increase in the substrate thickness causes their shifting to $\omega_N = (N + 0.5)\omega_d$. Notably, the same effect can be achieved by varying the 2DES density for a fixed substrate thickness, as illustrated in the figure by the plots of the normalized frequency versus the retardation parameter A :

$$A = \frac{2\omega_p}{\omega_d} = \frac{2}{\omega_d} \sqrt{\frac{n_s e^2}{(\varepsilon - 1)\varepsilon_0 m^* d}}.$$

In our experiments, $\varepsilon = \varepsilon_{\text{GaAs}} = 12.8$, and the data points at $A = 0.27$ and 0.83 are measured for the samples with the respective electron densities of $n_s = 1.4 \times 10^{11}$ and 1.4×10^{12} cm $^{-2}$. Both samples have the same substrate thickness $d = 0.2$ mm. In view of the given results, it is important to note that the dependency displayed in Fig. 1 has a universal character and applies to the substrates of an arbitrary thickness with any material used for the conducting film. To compare the experiment with theoretical prediction, Fig. 1 includes the solid curves corresponding to the theoretical approximation [14]

$$\omega_N = \frac{\omega_d}{2} \left(2N + \sqrt{\left(\frac{N}{1+A^2}\right)^2 + \frac{A^2}{1+A^2}} - \frac{N}{1+A^2} \right). \quad (3)$$

Thus, for instance, for the zero Fabry-Pérot maximum depicted in the blue color in Fig. 1, we obtain [14]

$$\omega_0 = \frac{\omega_d}{2} \frac{A}{\sqrt{1+A^2}}. \quad (4)$$

Here, it is worth noting that the approximation (3) yields

$$\omega_N = \omega_d \left(N + \frac{A^2}{4N} \right) \quad \text{at } A \rightarrow 0, \quad (5)$$

$$\omega_N = \omega_d \left(N + \frac{1}{2} - \frac{N}{2A^2} \right) \quad \text{at } A \rightarrow \infty. \quad (6)$$

Importantly, the shifting observed in Fig. 1 occurs *continuously*. As further discussion will show, it is indeed the hallmark of the limit $\omega\tau \gg 1$, when a conducting layer behaves as a 2D plasma. In our experiments in particular, $\omega\tau \approx 5$ for the wafer with electron mobility 100×10^3 cm 2 /V s at a frequency 0.2 THz.

In comparison to the plasmonic regime, it is instructive to investigate the behavior of Fabry-Pérot resonances in the opposite dirty limit of $\omega\tau \ll 1$. To accomplish that, we prepared a batch of samples fabricated from high-resistivity silicon, with a thin Cr layer evaporated on top of each sample. The thickness of the silicon substrate was fixed at $d = 0.4$ mm, while that of the Cr film was varied between the samples. For the Cr films under study the parameter $\omega\tau \approx 2 \times 10^{-4}$ at frequency 0.2 THz. Figure 2 shows the transmission spectra obtained for the samples with different values of 2D conductance σ_s measured at dc using the van der Pauw technique. The solid lines in the figure represent the theoretical prediction based on the Drude model [17]. As indicated by the data, for small values of the film conductivity $\sigma_s/(\varepsilon_0 c)$ the Fabry-Pérot resonances remain at their original positions $\omega_N = N\omega_d$. At the same time, an increase in 2D

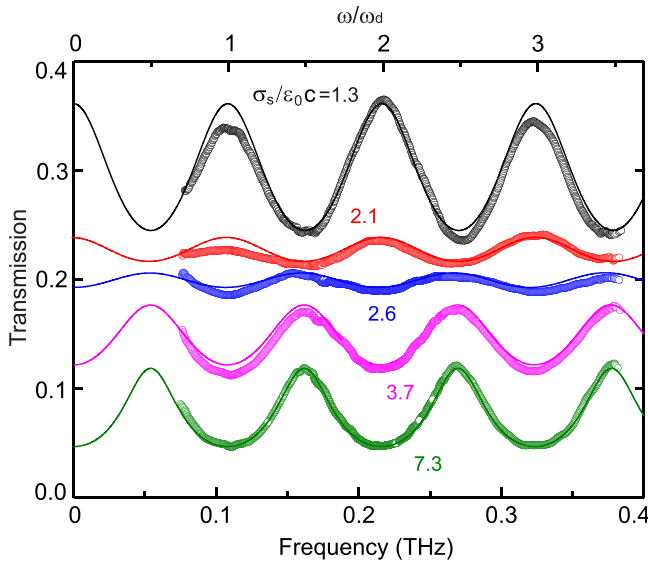


FIG. 2. Frequency dependence of the transmission through silicon samples with chromium films of different conductivities. The high-resistivity silicon substrate has the thickness $d = 0.4$ mm ($\epsilon_{\text{Si}} = 11.7$), and the Cr film thickness is varied in the range of 8–40 nm. The impedance matching phenomenon is observed at $\sigma_s/(\epsilon_0 c) \approx 2.35$, where the Fabry-Pérot resonances exhibit a π shift. The curves are plotted without offset.

conductivity results only in a reduction of Fabry-Pérot modulation amplitude. We observe that Fabry-Pérot oscillations nearly vanish at $\sigma_s/(\epsilon_0 c) \approx 2.35$. Most striking is that higher conductivity values lead to an abrupt phase reversal in the peak position. It is in stark contrast with the data in Fig. 1, where the shift undergoes continuously. A more detailed dependence of the normalized Fabry-Pérot peak position ω/ω_d on the conductivity $\sigma_s/(\epsilon_0 c)$ is plotted in Fig. 3. These mea-

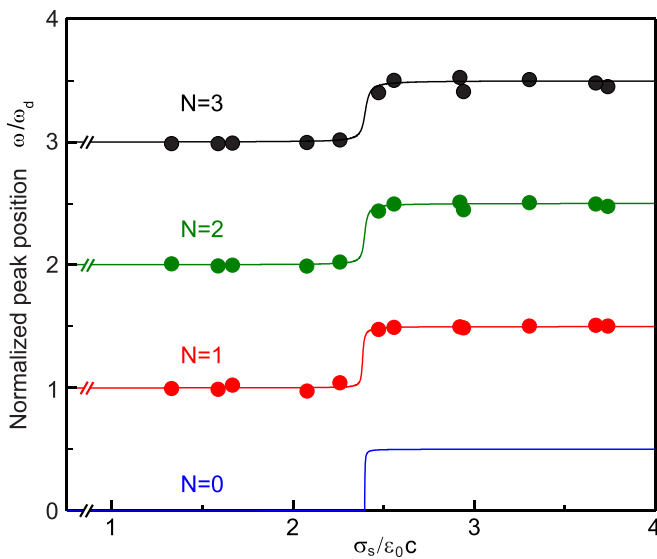


FIG. 3. Fabry-Pérot resonance frequency ω/ω_d plotted as a function of the chromium layer conductivity, $\sigma_s/(\epsilon_0 c)$. Experimental data do not include $N = 0$ Fabry-Pérot resonance due to the frequency restriction in the terahertz quasioptical setup.

surements are taken using 12 samples with the thicknesses of the chromium film in the range of 8–40 nm (see Supplemental Material for more details [17]).

IV. DISCUSSION

A thin metallic film can be regarded as an antireflection coating that works over an extremely wide-bandwidth terahertz range. For convenience, one can treat the propagating radiation from the wave-impedance perspective to understand the physics behind the discovered impedance matching phenomenon. In our case, the impedance of a wave propagating in a dielectric substrate, $Z_0/\sqrt{\epsilon}$, is loaded by the film and vacuum impedances R_s and Z_0 connected in parallel. Then, the impedance matching condition becomes

$$\frac{Z_0}{\sqrt{\epsilon}} = \frac{R_s Z_0}{R_s + Z_0}, \quad \frac{\sigma_s}{\epsilon_0 c} = \frac{Z_0}{R_s} = \sqrt{\epsilon} - 1. \quad (7)$$

The film conductivity can be described by the Drude formula $\sigma_s = \sigma_0/(1 - i\omega\tau)$, where $\sigma_0 = n_s e^2 \tau / m^*$. In the dirty limit, $\omega\tau \ll 1$, the 2D conductivity $\sigma_s = \sigma_0$ is frequency independent. Therefore, the relation (7) implies the absolute frequency independence of the impedance matching effect. For our experimental conditions, $\epsilon_{\text{Si}} = 11.7$, and the critical conductivity $\sigma_s/(\epsilon_0 c)$ is equal to 2.4, which is very close to the experimentally obtained value from the data in Fig. 2. Thus, the broadband nature of the present phenomenon is due to the fact that neither the wavelength nor the slab thickness enters the equations, because here the wave never travels through the conducting medium, but it sees it as an interface. For comparison, in optical antireflection coatings and Bragg mirrors the active role is played by the dielectric slab.

It is interesting to understand when a conducting layer can be treated as a 2D object in a particular type of experiment under consideration. Our calculations presented in the Supplemental Material [17] show that the film can be regarded as a 2D object when $h \ll d$ (h is the film thickness). In this case, all conclusions of the present paper are valid. An increase in the film thickness up to $h = 0.1d$ results only in a slight shift of the resonance frequency. Interestingly, that clean semiconductor slab, when $h = d$, still demonstrates a plasmonic response with a characteristic plasma frequency as in Eq. (1) with $n_s = n_{3D} d$.

V. CONCLUSION

In conclusion, we have investigated the sequence of Fabry-Pérot resonances in a dielectric slab with a conducting layer on one of the facets. As a result, two fundamentally different modes of the system electrodynamic response have been established. In the clean regime, $\omega\tau \gg 1$, the Fabry-Pérot resonances undergo a continuous shift in frequency, controlled solely by the retardation parameter $A \propto \sqrt{n_s d}$. In the opposite dirty limit, $\omega\tau \ll 1$, we observed an abrupt π shift at $\sigma_s/(\epsilon_0 c) = \sqrt{\epsilon} - 1$, when Fabry-Pérot oscillations completely disappear. Such a broadband impedance matching effect might be of interest in various terahertz applications. We have shown that the system electrodynamic in the dirty regime is governed by the dimensionless parameter $\sigma_s/(\epsilon_0 c)$.

ACKNOWLEDGMENTS

The authors gratefully acknowledge the financial support from the Russian Science Foundation (Grant No. 18-72-10072) and the Austrian Science Fund (I3456-N27).

-
- [1] C. Fabry and A. Perot, *Ann. Chim. Phys.* **16**, 7 (1899).
- [2] A. Perot and C. Fabry, *Astrophys. J.* **9**, 87 (1899).
- [3] E. Hecht, *Optics*, 2nd ed. (Addison-Wesley, Boston, 1987).
- [4] B. P. Gorshunov, G. V. Kozlov, A. A. Volkov, S. P. Lebedev, I. V. Fedorov, A. M. Prokhorov, V. I. Makhov, J. Schutzmann, and K. F. Renk, *Int. J. Infrared Millimeter Waves* **14**, 683 (1993).
- [5] B. P. Gorshunov, I. V. Fedorov, G. V. Kozlov, A. A. Volkov, and A. D. Semenov, *Solid State Commun.* **87**, 17 (1993).
- [6] M. Walther, D. G. Cooke, C. Sherstan, M. Hajar, M. R. Freeman, and F. A. Hegmann, *Phys. Rev. B* **76**, 125408 (2007).
- [7] N. Laman and D. Grischkowsky, *Appl. Phys. Lett.* **93**, 051105 (2008).
- [8] S. A. Kuznetsov, M. Navarro-Ca, V. V. Kubarev, A. V. Gelfand, M. Beruete, I. Campillo, and M. Sorolla, *Opt. Express* **17**, 11730 (2009).
- [9] N. Ubrig, I. Crassee, J. Levallois, I. O. Nedoliuk, F. Fromm, M. Kaiser, T. Seyller, and A. B. Kuzmenko, *Opt. Express* **21**, 24736 (2013).
- [10] S. D. Ganichev, S. N. Danilov, M. Kronseder, D. Schuh, I. Gronwald, D. Bougeard, E. L. Ivchenko, and A. Ya. Shulman, *J. Infrared, Millimeter, Terahertz Waves* **41**, 957 (2020).
- [11] M. Dressel and G. Grüner, *Electrodynamics of Solids: Optical Properties of Electrons in Matter*, 1st ed. (Cambridge University Press, Cambridge, UK, 2003).
- [12] Yu. A. Kosevich, *JETP Lett.* **53**, 150 (1991).
- [13] V. A. Volkov and V. N. Pavlov, *JETP Lett.* **99**, 93 (2014).
- [14] P. A. Gusikhin, V. M. Muravev, and I. V. Kukushkin, *Phys. Rev. B* **102**, 121404(R) (2020).
- [15] A. Shuvaev, V. M. Muravev, P. A. Gusikhin, J. Gospodarič, A. Pimenov, and I. V. Kukushkin, *Phys. Rev. Lett.* **126**, 136801 (2021).
- [16] G. Kozlov and A. Volkov, in *Millimeter and Submillimeter Wave Spectroscopy of Solids*, edited by G. Grüner, Topics in Applied Physics Vol. 74 (Springer, Berlin, 1998).
- [17] See Supplemental Material at <http://link.aps.org/supplemental/10.1103/PhysRevB.104.115408> for parameters of different Cr films and details of the used theoretical model.